RANS turbulence models for pitching airfoil

K. A. Ahmad, W. McEwan, J. K Watterson & J. Cole
Department of Aeronautical Engineering, Queens's University of Belfast, Belfast, UK

Abstract

The RANS code Fluent 6^{TM} is used to predict the flow field around a pitching NACA 0012 airfoil. Experimental data for this unsteady flow field is widely available for validation. A hybrid mesh was employed in the computational domain and different mesh configurations were tested and the results were compared. Several turbulence models such as k-ϵ and k-ω were tested and the results were also compared. The turbulence model that gives the best agreement with the experimental data is SST k-ω with y+ value set to 1. Mesh and time step dependence studies were also performed and it was found that the results were not affected by varying these parameters.

Nomenclature

c_l	Drag coefficient
c_d	Lift coefficient
c_m	Pitching moment coefficient
k	Turbulence kinetic energy
F^+	Reduced frequency
L	Length of the object
w	Natural frequency
y^+	Local Reynolds number
α	Angle of vibration
α_{max}	Maximum angle of pitch
α_{min}	Minimum angle of pitch
$d\alpha$	Range of the angle of pitch
ϵ	Dissipation rate of turbulence
ω	Specific turbulent dissipation rate

1 Introduction

Dynamic stall is an unsteady phenomenon that only occurs when lifting surfaces such as an airfoil pitch unsteadily to angles exceeding the static stall angle, causing the aerodynamic lift to increase beyond the maximum value for unstalled conditions. The aerodynamic forces and moment overshoots are usually associated with the formation of the dynamic stall vortex (DSV) which first appears at the leading edge of the lifting surfaces (in this case it is an airfoil) and travels along the lifting surfaces until it separates at the trailing edge. However, after the DSV detaches from the airfoil and moves into the wake, the lift decreases abruptly. Some researchers relate these overshoots to the delay of the separation rather than the formation of the dynamic stall vortex [1].

Over the past three decades, the dynamic stall phenomenon has been investigated through experimental and numerical approaches and significant progress has been made to understand the general features of the dynamic stall. Examples of past theoretical and experimental works can be found in Theodore [2], McCroskey [3], and Ohmi [4]. More recent experimental works can be found in Panda *et al* [5] and Coton *et al* [6]. Examples of numerical works can be found in the papers of Akbari [1], Carr [7], Tuncer [8], Ekaterianris [9], and Barakos [10]. These numerical studies have analysed the dynamic stall phenomenon in laminar and turbulent flow conditions.

In the present work, the dynamic stall characteristics of a pitching NACA 0012 airfoil were investigated. The RANS solver Fluent 6.1$^{\mathrm{TM}}$ was used to predict this unsteady flow problem. The objective of this investigation is to test the capability of Fluent to predict the dynamic stall phenomenon. Calculations were conducted with different turbulence models and near-wall treatments and the predictions were compared with previous experimental results [11].

2 Numerical method

The incompressible Reynolds-averaged Navier–Stokes (RANS) equations were modelled. This investigation focuses on the two-equation k-ϵ and k-ω turbulence models. The SIMPLE algorithm was used for pressure-velocity coupling and second order spatial discretization was used for all the equations.

2.1 Geometry, mesh and boundary conditions

Figure 1 shows a schematic diagram of the computational domain. The size of the computational domain was chosen in order to obtain a domain-independent solution.

A hybrid mesh was employed to ensure accuracy of the flow simulations near the wall surfaces. Quad cells were used around the airfoil while triangular cells were

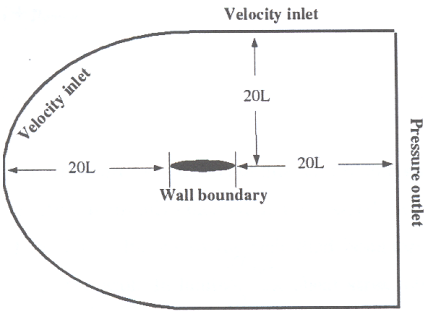

Figure 1: Computational domain of the pitching airfoil.

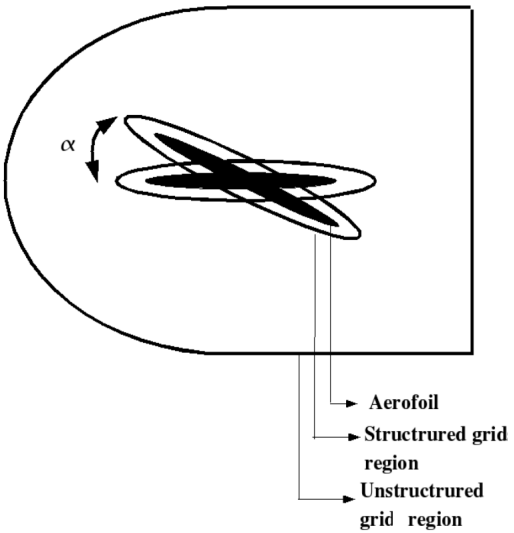

Figure 2: Rotating control domain for near-wall region.

used in the core of the flow. A mesh separation method was used so that when the airfoil rotates, its neighbouring quad cells also move with it. Hence the portion of quad cells remains unchanged thus maintaining the highest possible accuracy for the flow prediction near the wall (see Figure 2).

The prescribed pitching motion is based on the harmonic oscillation equations shown in the equation 1.

$$\alpha = \alpha_{min} + \frac{1}{2}(\alpha_{max} - \alpha_{min})(1 - cos(\omega t)) \tag{1}$$

The unsteady motion of the pitching airfoil is characterized by the reduced frequency of the oscillation. This is defined by equation 2. In the current study, the reduced frequency was chosen to be 0.15, the same as in the experiment.

Table 1: Two equations turbulence models with specified symbols.

Turbulence Model	Wall Treatment	No of cells	Symbol
k-ϵ	standard wall function	26670	kϵ I
	non-equilibrium wall function	26670	kϵ II
	two-layer near wall model	28370	kϵ III
reliazable k-ϵ	standard wall function	26670	rkϵ I
	non-equilibrium wall function	26670	rkϵ II
	two-layer near wall model	28370	rkϵ III
k-ω	standard wall function	26670	kω I
	two-layer near wall model	28370	kω II
SST k-ω	standard wall function	26670	SST kω I
	two-layer near wall model	28370	SST kω II

$$F^{+} = \frac{\omega L}{2u_{\infty}} \tag{2}$$

2.2 Testing condition and analysis

A time step of 1×10^{-3}sec was chosen and 60 sub-iterations per time step were performed.The Reynolds number, based on the freestream velocity was 1×10^{6}. The airfoil cycle starts at α=5^0 and the airfoil cycle amplitude is 20^0. The solutions were computed with four main turbulence models, namely the k-ϵ, realizable k-ϵ, k-ω, and SST k-ω. Each turbulence model is tested with two or three different wall treatment approaches. If a wall function is used, then the wall y^+ value will be in the range of 30 to 60, whilst if a wall function is not in used, the wall y^+ approaches 1. Table 1 shows all the turbulence models that were used with their symbols. Calculations were run for several cycles until periodicity was observed in the solutions. The simulations were performed using a serial version of Fluent code and time taken for most cases took about 72 hours on a Intel Pentium IV 2.66GHz.

3 Result

3.1 Validation of RANS turbulence models

Results for k-ϵ and rk-ϵ are shown in Figure 3. The lift coefficient values for k-ϵ I and II were predicted well for the early upstroke stage, but both models performed poorly when the airfoil approached 25^0 and during the downstroke cycle. The c_d and c_m plots (see Figure 3 ((b)-(c))) show that both models delay the

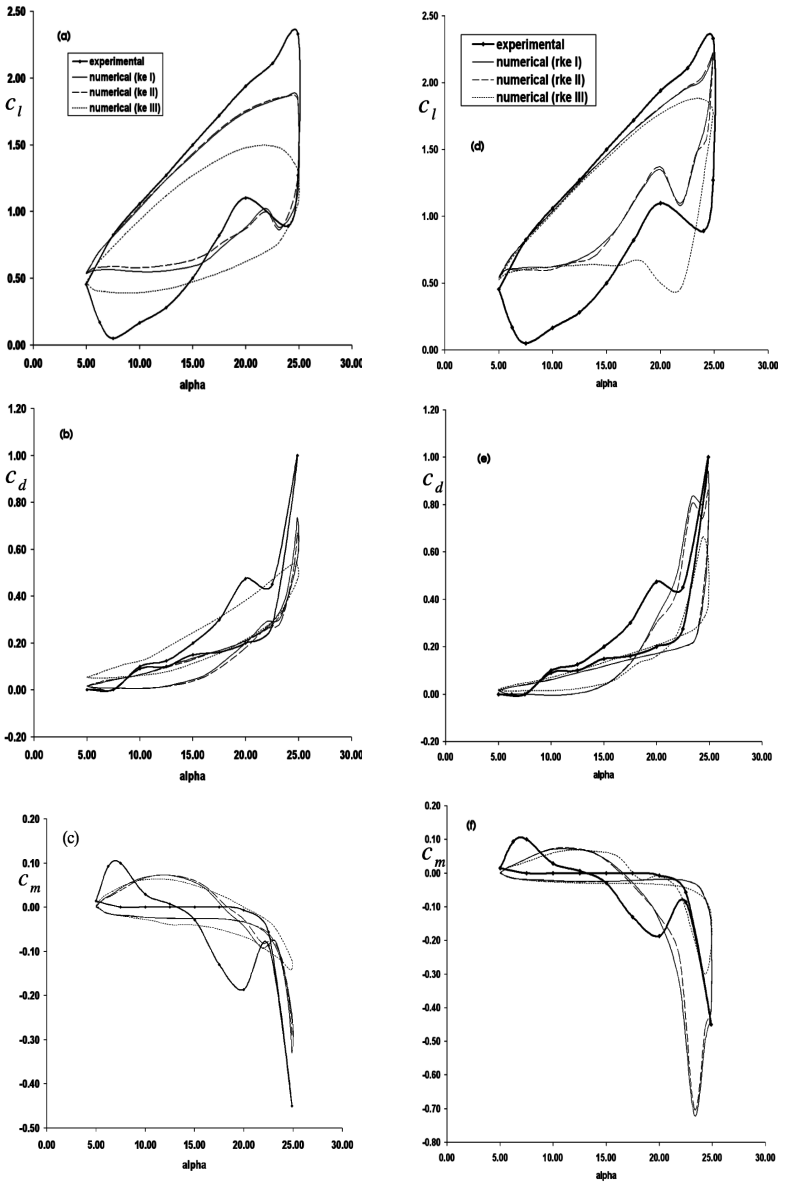

Figure 3: Hysteresis loops for k-ϵ ((a)-(c)) and rk-ϵ((d)-(f)).

DSV separation (notice that the rapid increase in predicted values of c_d and c_m was delayed). It can be concluded that k-ϵ model does not have the capability to predict the nature of the dynamic stall. Meanwhile, the rk-ϵ I and II models managed to predict the essential features for the upstroke stage (see Figure 3((d)-(f))). However, the difference between the experimental results and the rk-ϵ I and

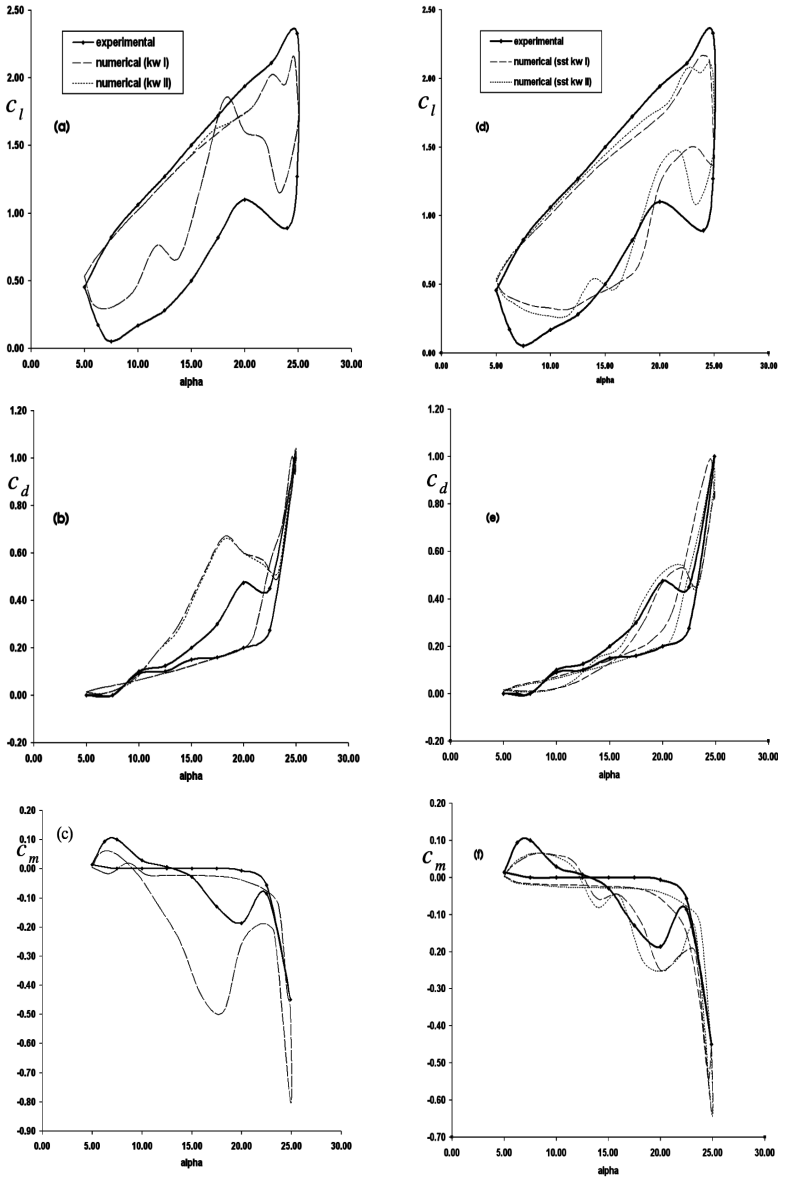

Figure 4: Hysteresis loops for k-ω ((a)-(c)) and SSTk-ω((d)-(f)).

II remains large for the high angle of attack. Nevertheless, both models managed to capture the formation and the detachment of the trailing edge vortex at the early stage of the downstroke. It is also clear that the rk-ϵ gives better agreement compared to standard k-ϵ. This superior performance is more pronounced in the c_l hysteresis loop. These trends were expected as rk-ϵ is designed to improve

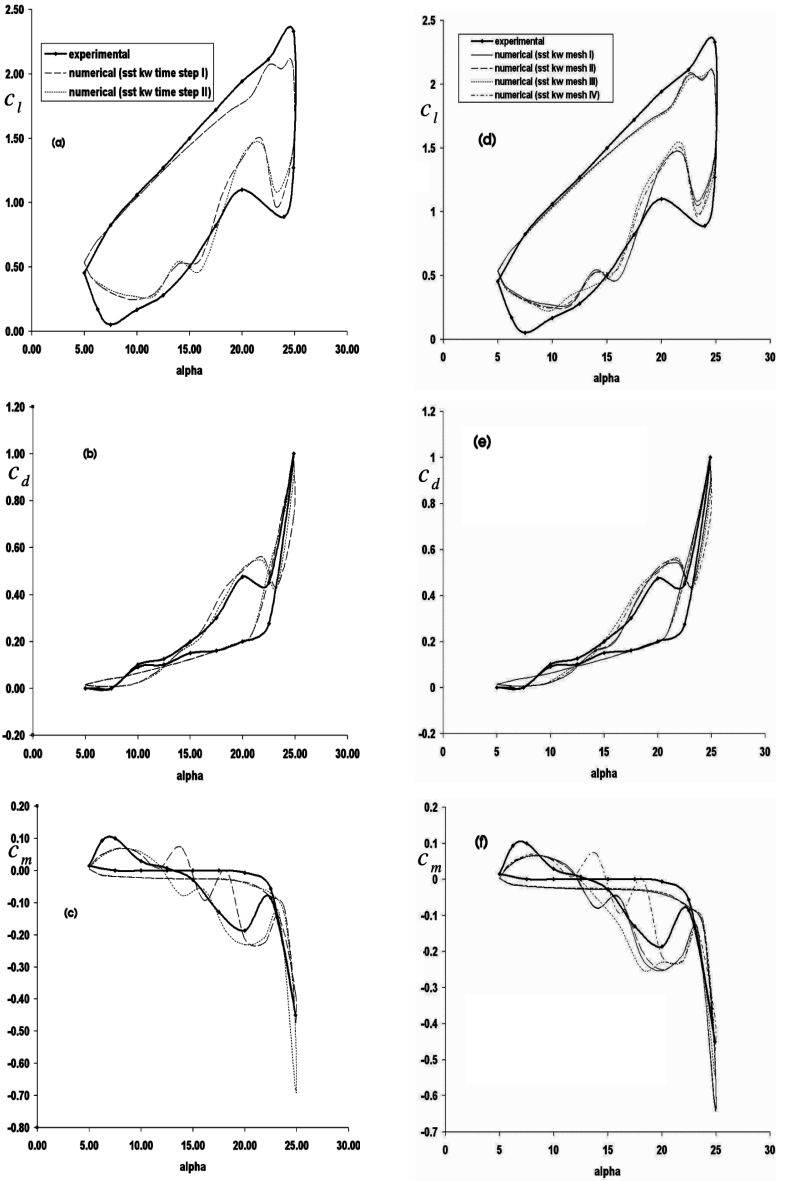

Figure 5: Solutions dependency study.

computations of separated flows. One also can see that having y^+ value equal to 1, did not help to improve the predictions.

Figure 4 shows the lift, drag, and pitching moment hysteresis loops for k-ω and SST k-ω turbulence models. From the figures (see Figure 4 ((a)-(c))), it can be seen that the k-ω I and II managed to capture the trend of the hysteresis loops.

Table 2: Various mesh size with specified symbols.

Turbulence Model	Mesh Size	Symbol
SST k-ω	28370	sst kω mesh I
	52573	sst kω mesh II
	78627	sst kω mesh III
	109025	sst kω mesh IV

Both models give reasonable agreement with the experimental data during the upstroke stage, but differed significantly for the downstroke stage. The lift overshoot during the downstroke stage probably was caused by the formation of a strong trailing edge vortex. This second vortex initially grows in size and then detaches from the airfoil surface and convects in the wake. The drag hysteresis loop shows that there was an early separation of DSV from the airfoil surface. Overall performance of both models are sufficient to predict the mean features of the dynamic stall phenomenon. Although the difference between computation and experimental data remains large, the general features of the flow are predicted reasonably well.

Meanwhile Figure 4 ((d)-(f)) show that SST k-ω I and II predictions are in good agreement with the experimental results for the upstroke stage. In fact, the difference is smaller compared to the other turbulence models that have been tested. The SST k-ω I model predicts the lift overshoot nearly the same as the experiments. However, this model still fails to predict the formation of the trailing edge vortex. Meanwhile the SST k-ω II managed to predict the formation of the trailing edge vortex and its detachment. From the c_m hysteresis loop (see Figure 4 (f)), it can be seen that SST k-ω delays the separation of the dynamic stall vortex.

Overall performance is satisfactory especially for SST k-ω II turbulence model. This turbulence model will be used for all the 2D computation in the remainder of this work.

3.2 Time step and mesh dependency analysis

Figures 5((a) to (c)) show the hysteresis loops for SST k-ω with the time step of 1×10^{-3} sec (SST k-ω time step I) and 5×10^{-4} sec (SST k-ω time step II). One can see that varying the time step value, does not significantly affect the computational results. However, for the c_m value, the lower time step gives a more stabilized solution with fewer oscillations during the downstroke stage.

Table 2 shows the symbols used for each model with different mesh size while figures 5((d) to (f)) show the hysteresis loops of various mesh size. The refinement of the mesh is focused on the suction surface of the airfoil as most of the crucial elements of the dynamic stall phenomenon occur on this surface. From these figures, it can be clearly seen that there is no significant change during the upstroke stage.

The c_l loop shows that the increment of the mesh will reduce the gap between the computational and experimental results at the beginning of the downstroke stage. This increment also induces oscillations of c_l and c_m during the downstroke stage.

It must be observed that the time step and mesh independent predictions of the c_m hysteresis loop have not been obtained. This implies that the predicted pressure distribution and evolution of the DSV are not time step or mesh independent.

4 Conclusion

A RANS code has been used to predict the flow field around a pitching NACA 0012 airfoil.The results demonstrated that the best turbulence model that gives the best agreement with the experimental data is SST k-ω with y+ value is set to 1. It was also found that the c_l and c_d were not effected by varying the time step and mesh parameters. However it was observed that time step and mesh independent predictions for the c_m hysteresis loop could not be obtained.

References

[1] Akbari, M.H., Price, S.J., "Simulation of dynamic stall for a NACA 0012 airfoil using a vortex method", Journal of Fluids and Structures 17 (2003) pp. 855-874.

[2] Theodorsen, T., "General theory of aerodynamic instability and the mechanism of flutter", Report National Advisory Committee for Aeronautics, report no 496.

[3] McCroskey, W.J.,"Some current research in unsteady fluid dynamics-the 1976 freeman scholar lecture", Journal of Fluids Engineering, pp 8-39, 1977.

[4] Ohmi, K., Coutanceau, M., Daube, O., Loc, T.P.,"Further experiments on vortex formation around and oscillating and translating airfoil at large incidences", Journal of Fluid Mechanics, pp 607-630, vol 225, 1991.

[5] Panda, J., Zaman, K.B.M.Q., "Experimental investigation of the flow field of an oscillating airfoil and estimation of lift from wake surveys",Journal of Fluid Mechanics, Vol. 265, pp. 65-95, 1994.

[6] Coton, F.N., Galbraith, R.A.M., JIang, D., and Gilmour.,"An experimental study of the effect of pitch rate on the dynamic stall of a finite wing", Unsteady aerodynamics two days conference, Royal Aeronautical Society, 17-18 July 1996.

[7] Carr, L.W., "Progress in analysis and prediction of dynamic stall", AIAA Atmospheric Flight Mechanics Conference, Snowmass, CO, August 19-21, 1985.

[8] Tuncer, I.H., Wu, J.C., Wang, C.M., "Theoretical and numerical studies of oscillating airfoils", AIAA Journal, no. 9, Vol. 28, Sept 1990.

[9] Ekaterinaris, J.A., Menter, F.R., "Computation of oscillating airfoil flows with one and two equation turbulence models", AIAA Journal, no 12, Vol. 28, Dec 1994.

[10] Barakos, G.N., Drikakis, D., "Unsteady separated flows over manoeuvring lifting surfaces", Phil. Trans. R. Soc. Ion. a(2000) 358, 3279-3291
[11] McCroskey, W.J., McAllister, K.W., Pucci, S.L., Carr, L.W., "An experimental study of dynamic stall on advanced airfoil sections, pressure, and force data", NASA TM-84245, vol. 2, Sept. 1982.